Controlling Light by Curvilinear MetaSurfaces

AbdelMajid Taibi
School of Engineering and the Built Environment, Edinburgh Napier University
United Kingdom
m.taibi@napier.ac.uk

Antoine Durant
IUT1 - Electrical Engineering and Industrial Computing, Université Grenoble Alpes
France
antoine.durant@etu.univ-grenoble-alpes.fr

Valeria Loscrí
Inria Lille-Nord Europe
France
valeria.loscri@inria.fr

Anna Maria Vegni
Department of Engineering, Roma Tre University
Italy
annamaria.vegni@uniroma3.it

Luigi La Spada
School of Engineering and the Built Environment, Edinburgh Napier University
United Kingdom
l.laspada@napier.ac.uk

ABSTRACT

Huge interest in controlling and manipulating electromagnetic waves is recently and strongly evolving, mainly due to the growing demand of reliable technologies in several application fields, such as communications, healthcare, military and safety. Despite the plethora of technologies existing nowadays, limitations are still present, such as limited speed, low response control, narrow bandwidth, and large dimensions of electronic devices. In this scenario, new engineered materials with unprecedented electromagnetic properties (*i.e.*, MetaSurfaces) can represent a very suitable technology solution.

In this paper, a MetaSurface structure is modelled, designed, manufactured and experimentally tested, to be used in several applications. Specifically, results are presented for (*i*) advanced medical diagnostics, (*ii*) enhance communication signals along curvilinear paths (*i.e.*, bend optical fibers) and (*iii*) cloaking applications. Experimental results reveal that the MetaSurface can fully manipulate and process electromagnetic waves at will. The proposed structure appears to be highly versatile and scalable, with great potential to be used for many other practical applications.

KEYWORDS

MetaSurface, Sensing, Communications

ACM Reference Format:
AbdelMajid Taibi, Antoine Durant, Valeria Loscrí, Anna Maria Vegni, and Luigi La Spada. 2019. Controlling Light by Curvilinear MetaSurfaces. In *NanoCom'19: 6th ACM International Conference on Nanoscale Computing and Communication, September 25–27, 2019, Dublin, Ireland.* ACM, New York, NY, USA, 6 pages. https://doi.org/10.1145/1122445.1122456

NanoCom'19, September 25–27, 2019, Dublin, Ireland

ACM ISBN 978-1-4503-9999-9/18/06…$15.00
https://doi.org/10.1145/1122445.1122456

1 INTRODUCTION

Manipulating electromagnetic waves recently attracted great attention in different industrial sector [1–3] *i.e.*, telecommunications, computing and storage data, sensing and diagnostics. Traditional designs have been extensively used, such as interferometers, waveguides, gratings, plasmonics, cavities/resonators, and the most recent Metamaterials [4]. Even if they possess some advantages (*i.e.* speed, low-cost, high sensitivity and selectivity), some limitations are still present like the relatively large physical dimensions, high losses and not easy to be manufactured [5].

Leveraging on such considerations, MetaSurfaces [6] have found great potential in controlling and manipulating electromagnetic waves at will. Such materials are composed of metallic or dielectric inclusions, either periodically or randomly dispersed in an array configuration, whose physical dimensions and spatial periodicity are much smaller as compared to the operative wavelength. They present further advantages as compared to their Metamaterial counterpart such as (*i*) the reduction of undesirable losses and real-time response control [7], (*ii*) advanced integration and miniaturization [8], that makes the fabrication process readily achievable for many on-chip applications, and (*iii*) the scalability and implementation among different frequencies from microwave to optics [9]. Despite such advantages, electrically ultrathin MetaSurfaces (*i.e.*, thickness much smaller than wavelength) cannot fully manipulate wave, due to the fact they exhibit intrinsic losses, narrow bandwidth operation, limited scattering cross sections, and low efficiency. For this reason, in this work a new designed and manufactured material, namely, Curvilinear MetaSurface, will be presented. It aims to control wave properties over arbitrary shape objects to realize practical devices for communications and sensing applications.

This paper is organized as follows. In Section 2, we first evaluate the MetaSurface electromagnetic properties through its Impedance Z and admittance Y distribution; then, we link them with its physical dimensions. Once the MetaSurface is properly developed, an overview of the manufactured MetaSurface structure will be presented in Section 3, along with the experimental setup used to test it. In Section 4, the realized MetaSurface will be experimentally tested for different purposes *i.e.*, (*i*) high sensitivity and selectivity sensors and imaging systems for advanced medical diagnostics;

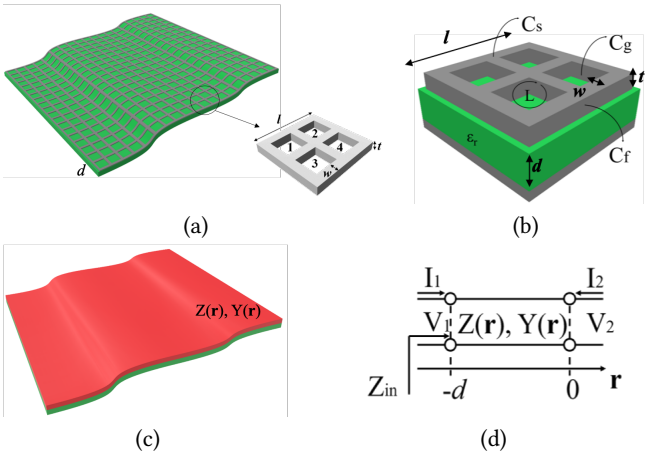

Figure 1: (a) Curvilinear MetaSurface deposited on an homogeneous dielectric slab; (b) Unit-cell and dimensions *i.e.*, l side-length, w strip width, t thickness, d slab thickness, ε_r substrate permittivity; (c) Equivalent dielectric multi-layer model; (d) Non-Uniform-Transmission-Line (NUTL) model for Curvilinear MetaSurfaces.

(*ii*) enhance transmission channels and signals across sharp and bent corners; (*iii*) cloaking of 3D objects for defense and military applications. Finally, conclusions are drawn at the end of the paper.

2 MATERIALS AND METHODS

In this section, we aim to link the propagation properties of the impinging wave with electric **E** and magnetic **H** components, with the structure electromagnetic characteristics (*i.e.*, constitutive parameters) through its Impedance and Admittance $Z(\mathbf{r})$ and $Y(\mathbf{r})$, respectively. As previously mentioned, electrically ultrathin MetaSurface, based on arrays of metallic inclusions and their Babinet-inverted counterparts are not fully reliable in light manipulation and processing. Since the aim of this paper is to achieve a full wave propagation control, the MetaSurface is considered having finite (yet small) thickness.

Let us consider a curved MetaSurface structure as the one depicted in Figure 1 (a). It is composed by patches as the ones in Figure 1 (b), either metallic or dielectric, deposited on a grounded dielectric substrate. For simplicity, the slab has thickness t, homogeneous permittivity ε_{slab} and permeability equal to that one of the free-space *i.e.*, $\mu_{slab} = \mu_0$. The top layer is air with permittivity ε_0 and permeability μ_0, from where the electromagnetic wave impinges with an incident angle θ_i.

Since the MetaSurface has a finite thickness, we can model it as a non-homogeneous dielectric slab of permittivity $\varepsilon(\mathbf{r})$ and/or magnetic permeability $\mu(\mathbf{r})$ as depicted in Figure 1 (c), where $\mathbf{r}$ is the position vector. By using Non-Homogeneous Transmission-Line Model (NHTLM), either the electric or magnetic component can be described as voltage $V(\mathbf{r})$ and current $I(\mathbf{r})$, respectively, as depicted in Figure 1 (d):

$$\begin{cases} \dfrac{\partial V(\mathbf{r})}{\partial \mathbf{r}} = Z(\mathbf{r})\, I(\mathbf{r}) \\ \dfrac{\partial I(\mathbf{r})}{\partial \mathbf{r}} = Y(\mathbf{r})\, V(\mathbf{r}) \end{cases} \tag{1}$$

Once we know the Impedance $Z(\mathbf{r})$ and Admittance $Y(\mathbf{r})$ distributions, we need to relate them to the real structure physical properties (namely, substrate thickness, inclusions dimensions and spatial periodicity). To evaluate the total impedance of the structure, let us break-down the design process in three main elements to design, each of them plays a crucial role in the manipulation and processing of the wave. As known, when a wave is impinging on metallic (dielectric) patches, a time-varying magnetic (**H**) component (in the direction perpendicular to the surface of the unit-cell) and an electric (**E**) component (in the dielectric gaps) are both produced. Along the structure, currents are induced by such components, namely the electric $\mathbf{J_e}(\mathbf{r}) = \mathbf{n} \times \mathbf{H}(\mathbf{r})$, equivalent magnetic $\mathbf{J_m}(\mathbf{r}) = -\mathbf{n} \times \mathbf{E}(\mathbf{r})$ and electric displacement $\mathbf{J_d}(\mathbf{r}) = \varepsilon(\mathbf{r})\mathbf{E}(\mathbf{r})$. We can relate the vector components (*i.e.*, electric $\mathbf{E}(\mathbf{r})$, magnetic $\mathbf{H}(\mathbf{r})$ and currents $\mathbf{J}(\mathbf{r})$) to their circuit elements counterparts (*i.e.*, voltage V, current I, Resistance R, Inductance L, and Capacitance C). Therefore, the related Impedance Z (Admittance Y), depicted in Figure 2 (b), reads [13]:

$$Z_{unit-cell} = \frac{j\omega L_{tot}}{1 - \omega^2 L_{tot} C_{tot}}. \tag{2}$$

For a single-layer ultrathin MetaSurface, only transverse currents are induced, symmetrically radiating on both sides of the MetaSurface and limiting the efficiency of the device. Therefore, a single ultrathin MetaSurface is equivalent to a shunt (parallel) reactance, which can only introduce a discontinuity on the transverse magnetic field. To determine a discontinuity also on the transverse electric field, it is necessary to introduce an impedance element in series by using a separation layer, typically a dielectric substrate, as depicted in Figure 2 (c). In this way all the boundary conditions are fully satisfied *i.e.*, parallel and series impedances form T- or Π-network circuit, whose impedance, shown in Figure 2 (d), is:

$$Z_{tot} = \frac{Z_{unit-cell} X_c}{Z_{unit-cell} + 2X_c}. \tag{3}$$

Finally, in previous works it has been assumed that coupling phenomena was detrimental in controlling the wave phase. Here, on the contrary, where the focus is the control of amplitude and phase at the same time, both intra- and inter -layer couplings cannot be neglected. In presence of more than one structure (Figure 2 (e)), the adjacent structures result magnetically and/or electrically coupled. In Figure 2 (f), the coupling phenomena are equivalent to mutual inductance Z_M and/or mutual capacitance Z_C, respectively as [15]:

$$Z_M = j\omega L + \frac{j\omega L Z_{tot} k^2}{j\omega L + Z_{tot} k^2}, \tag{4}$$

and

$$Z_C = \varepsilon_{sub} l \frac{K\left(\sqrt{1-k^2}\right)}{K(k)}. \tag{5}$$

Finally, we relate the circuit elements of the impedance (*i.e.*, resistance, inductance and capacitance) to the physical dimensions of the structure. Their evaluation is strictly related to the structure shape/geometry and the frequency range used: they are called

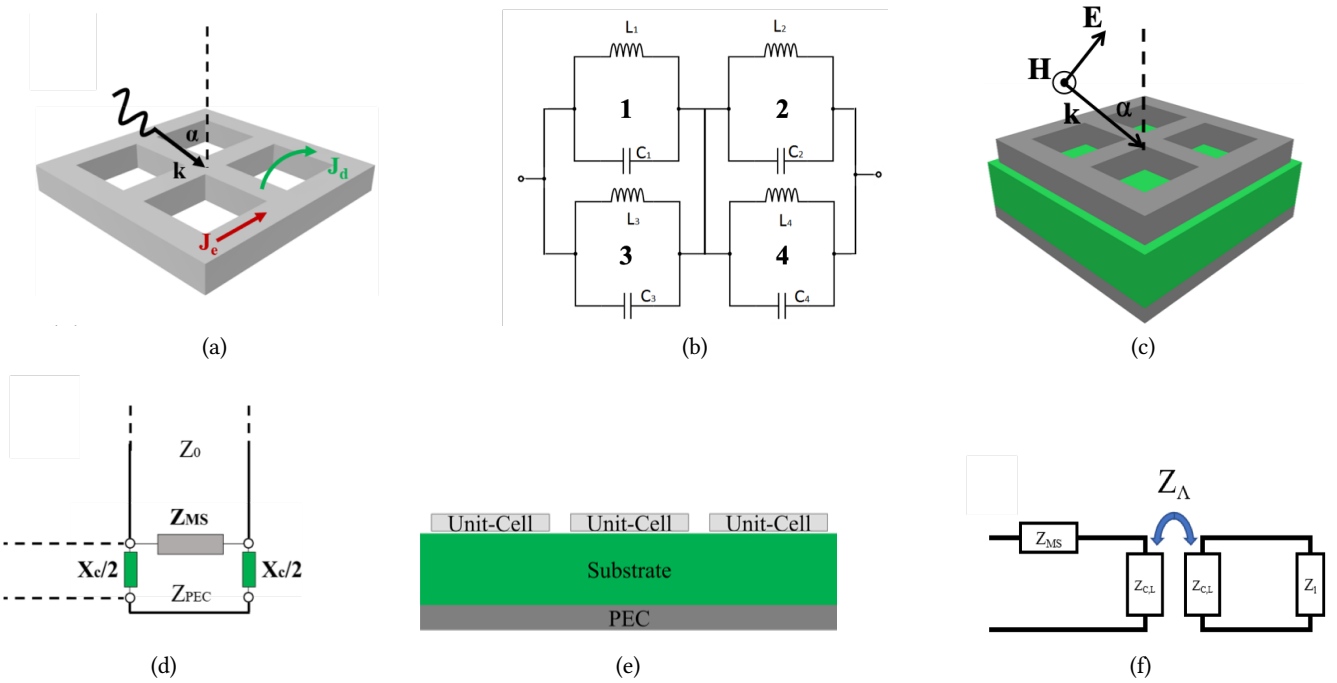

Figure 2: Unit-cell features: (a) Top Metallic (Bottom dielectric) layer; (b) Equivalent Circuit Model; (c) Perspective view of the unit-cell; (d) Full Impedance Model; (e) Side-view of the MetaSurface structure with adjacent cells; (f) Intra- and Inter- layer coupling effects equivalent circuit model.

"geometrical" and "additional" terms, respectively. Regarding the geometrical terms, by using formulas coming from electro-statics [13] and magneto-statics [14], both capacitance and inductance can be evaluated. The total inductance can be written as the sum of two contributions *i.e.*, (*i*) the self-inductance L_{self} of the loop and (*ii*) the mutual inductance M between the three-dimensional arms of the structure *i.e.*, $L_{tot} = L_{self}(l, w, t) - 4M(l, l - w)$, where l is the square side length, t the metal thickness and w the strip width.

The total capacitance can be expressed, instead, as the contribution of three different terms *i.e.*, $C_{tot} = C_g(w, t, g) + C_f(w, g) + C_s(l, w, t, g)$, with C_{gap} as the gap/slot parallel plate capacitance (*i.e.*, g is the gap distance), $C_{fringing}$ representing the contribution of the electric field lines connecting the two gap/slot plates, and $C_{superficial}$ for the charges on the ring surface. Regarding the additional terms, especially at the higher frequencies considered here (*i.e.* THz and Infrared), additional energy is stored within the metal: the inductive inertia of the electrons oscillating in the metal and the electron potential energy created by separate charges within the metal, described by an inductive $X_{L_{add}} = j\omega L_{add}(l, w, t)$ and capacitive $X_{C_{add}} = 1/j\omega C_{add}(l, w, t)$ reactance, respectively [15].

3 MANUFACTURING AND EXPERIMENTAL CHARACTERIZATION

So far, passive MetaSurfaces with infinitesimal thickness can manipulate the wave phase with low manipulation capabilities for the amplitude [16]. A possible solution, to achieve slightly higher control is the use of isotropic cascaded layers [17]. Unfortunately, such designs generally require very sophisticated fabrication processes, mainly relatively big unit-cells dimensions, complicated shapes and not easily scalable and reusable among different frequency ranges. The manufacturing technique used here is different from approaches existing in literature. Such techniques are usually expensive and restricted to a small area, and is not readily scalable, especially for complex shapes. The problem is due to the fine size required for the wavelengths of operation. In this work, instead, we fabricated and experimentally demonstrated a flexible curvilinear MetaSurface, whose properties are dictated by both modeling and design requirements (*i.e.*, Impedance Z, Admittance Y). Such a new fabrication technique allows full control of mesh size when going from a flat structure to the wanted curvilinear shape; and it results extremely useful and of crucial interest in many practical industrial sectors. Moreover, the same process can be used for different frequency ranges and replicated for any size and shape.

The MetaSurface consists of two physically separated non- homogeneous layers *i.e.*, the top layer is an array of metallic square-shaped particles, instead the bottom layer is its dielectric counterpart. The conductive grid is facing towards the air region, and the dielectric one is facing towards the slab region. The two layers are separated by a homogeneous dielectric substrate of permittivity $\varepsilon_r = 15$. The manufacturing process can be divided into three distinct stages [13] *i.e.*, (*i*) creation of the grid pattern to obtain the control of the unit-cell (see Figure 3 (a)); (*ii*) deposition on the

dielectric substrate to tailor the thickness effects; (*iii*) vacuum forming of the curvilinear shape to manage the intra- and inter- layers couplings (Figure 2 (b)).

The device has been, then, characterized by using the following experimental setup (Figure 3 (c)): the MetaSurface device is illuminated by an electromagnetic source typically waveguide-like attached to a network analyzer. To detect the output signal along the device, an NSI planar scanner has been used with a probe positioned closely to the MetaSurface device. An absorbing layer is used to bound the entire structure to reduce reflections at the boundaries along the xy-plane. With this two-port set up (*i.e.*, port 1 the source, port 2 the probe), both the reflection and transmission parameters are measured for the device. After the data are acquired, further processing is performed by using a similar spectral analysis conducted in [17]. This has the purpose to decompose the complex signals into simpler parts, namely radiated, guided and surface waves. The measured performances agree very well with both simulations and theory results, predicted by the modeling and design approach.

4 RESULTS AND DISCUSSION

In this section, we experimentally demonstrate how the manufactured MetaSurface can be used for different purposes and applications *i.e.*, sensing, communications and cloaking.

4.1 Refractive index and Absorption Measurements in sensing and medical diagnostics

The primary aim of an electromagnetic sensor is to produce an output signal, related to the type and/or concentration of the sample under study. Diseases in biological samples typically induce structural, biochemical and mechanical variations, implying significant modifications in their refractive index and absorption properties [19]. In other words, the specific disease generates a change in the electromagnetic properties of the sample under study. The main aim of the electromagnetic biosensor is to reveal such differences, by correlating the sample properties to the output signal characteristics: frequency, amplitude and bandwidth. Micro and nano biosensors have been recently used for this purpose [20]: simplicity, speed, low-cost, integration and label-free analysis are their main advantages. Considering the wide range of materials/samples to investigate, electromagnetic sensors should have additional performance requirements such as: high sensitivity and selectivity, bio-compatibility and immunity to external disturbances.

In this scenario a crucial role is played by MetaSurface-based sensors. They operate in the red- and near- infrared (NIR) range of the electromagnetic spectrum, for two main reasons: first, existing technologies are bound to the available and commercial laser diodes; secondly, most of biological material is supposed to induce less interferences when detecting in the NIR region, compared to the microwave and visible range. There are further advantages in using MetaSurface as sensors: they do not require markers to be attached to the analyte molecules; due to the high confined and localized field, they can be miniaturized and spatially multiplexed for sensing multiple substances at the same time, maintaining a fast-response. By using the proposed design and manufacturing technique, we realize an IR sensor for advanced sensing and medical diagnostics.

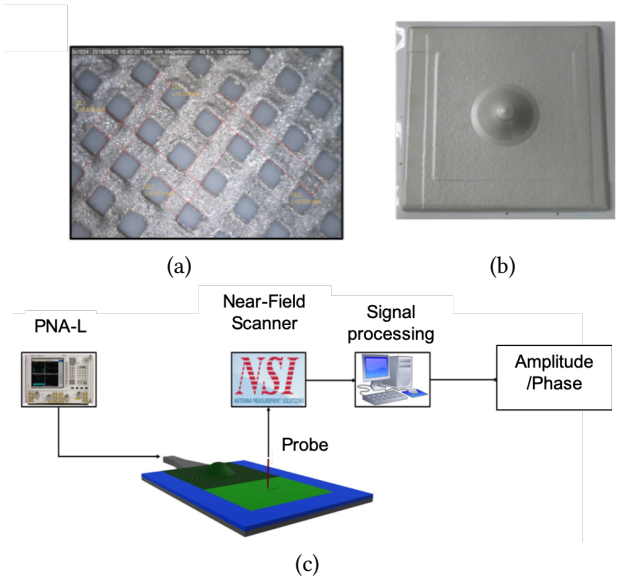

Figure 3: (MetaSurface manufactured: (a) planar grid pattern creation and deposition on dielectric substrate; (b) vacuum forming of the curvilinear shape; (c) experimental setup used to characterize and test the realized MetaSurface.

The aim of the MetaSurface is to correlate the sample properties (diseases) to the reflection/transmission coefficients characteristics (amplitude, phase, bandwidth) coming from the MetaSurface. Let us consider the structure of Figure 2: the top-layer is made of a Split-Ring-Resonators (SRRs), the bottom one is composed by its complementary counterpart (Babinet-inverted) Complementary-SRR (CSRR), separated by a homogeneous dielectric substrate. The structure Impedance is obtained by following the proposed method, and consequently fabricated by using the manufacturing process *i.e.*:

$$Z_{structure} = Z_{tot}\sqrt{1-\frac{\sin^2\alpha}{X_c}}\tan\left(\frac{\omega}{c}Z_{tot}d\right). \qquad (6)$$

From the practical point of view, to detect biological alterations, we made use of two sensing platforms [12]:

(1) **Refractive-index measurements** [21], Figure 4(a): The device itself possesses a specific response in terms of frequency position, amplitude and phase. Once the sample to study is placed in contact, the overall device characteristics change as a function of the sample properties. From the frequency position of the resonant dip, it is possible to discern the substance that we are looking for. Example of a sensor for glucose concentration measurements is depicted in Figure 4 (b).
(2) **Absorption measurements**, Figure 4 (c): The sensor is placed at a specific distance from the sample. Unlike the previous situation, changes are detected in the transmission coefficient magnitude and amplitude width, while the resonant wavelength position does not change. From the resonance magnitude and bandwidth, we reveal the sample

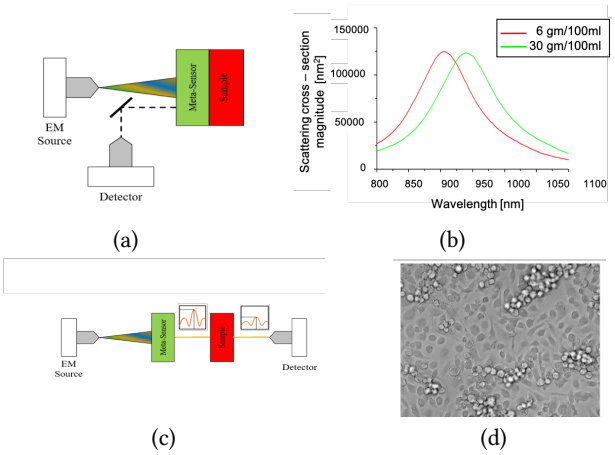

Figure 4: (a) Refractive-Index measurement setup; (b) glucose detection in human bloodstream for different concentrations; (c) absorption measurements setup; (d) imaging result for BMM cells detection.

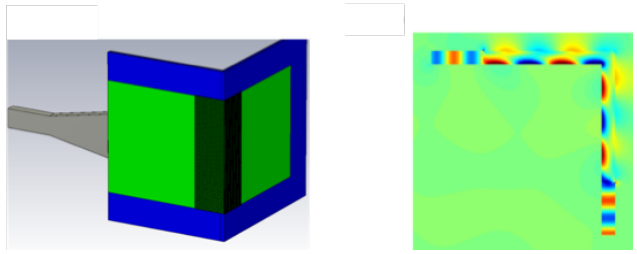

Figure 5: (a) Experimental Setup used to test a sharp corner (90-degrees) waveguide; (b) 2D electric field distribution of both guided- and surface- wave along the waveguide structure under test.

type and concentration. To this regard, an enhanced imaging system to detect mouse BMM cells (Bone Marrow derived Macrophages) in culture [22, 23], based on their absorption properties, has been developed (Figure 4 (d)).

4.2 Guiding waves around corners

Waveguides and optical fibers are crucial components in integrated circuits and communication technologies. Structures encountered in practice often exhibit sharp wedges, vertices, or corners. The presence of any abrupt discontinuities typically leads to pronounced losses and consequently high attenuation of the propagating wave. The possibility to guide electromagnetic waves around corners and/or discontinuities, without affecting their amplitude and phase, results of great importance in such systems. Despite the technology advancements and the variety of achievable devices [24], several problems are still present, mainly (but not limited to): fixed/narrow operational bandwidth; connectors geometry and dimensions; complexity in realizing specific refractive index values for core and cladding structures. Manipulating guided-waves by using MetaSurfaces is crucial to develop devices for nano-communications and military applications, especially where it is important to carry stronger signals with higher bandwidth and transmission rates as compared to their counterparts such as optical fibers. Moreover, it will be possible to develop new high-speed circuits (fast transmission and data processing), and at the same time reduce dissipation problems for short- and long-range communications. To bend electromagnetic waves around discontinuities (sharp 90-degrees corners), we divided the structure it in three different sub-sections (Figure 5 (a)), and then we manufactured the curvilinear non-homogenous MetaSurface, accordingly. Sections 1 and 3 are treated as planar dielectric slab, whose Electric Field pattern is well-known [25].

Section 2 is the curvilinear section whose Impedance can be found, starting from the Impedance profile, by using the following Elliptical Cylindrical Coordinates (μ, ν, z) Transformation:

$$\begin{cases} x = a \cosh \mu \cos \nu \\ y = a \sinh \mu \sin \nu \\ z = z \end{cases} \tag{7}$$

Simulations and experimental results are shown in Figure 5 (b). In Section 1 the energy is trapped inside the slab, the wave propagates with a constant velocity along the propagation direction, forming a standing wave. At the corner the incidence angle drastically, modifying direction, wave velocity, and the wave pattern across the slab. For the wave pattern across the entire slab to remain the same along all the curvature all multiple reflected waves must add in phase. The structure is made of both metallic and dielectric patterns: this determines a special boundary condition named Perfect-ElectroMagnetic Conductor (PEMC) [26], where the PEC is sustained by the High Impedance structure (top metallic layer) and the PMC is developed by the Low Impedance one (dielectric layer). In analogy to fluid-dynamics, we can see the curvilinear MetaSurface channel (around the sharp corner) acting as a narrow pipe connecting two straight conduits. To go through this tight channel, fluids should increase velocity to maintain constant the flux (mass transported across the cross section). In a similar way, the electromagnetic energy transported across the cross section must remain constant, therefore the velocities of the wave components should change locally (faster externally where the curvature is larger, slower internally where the curvature is smaller): in this way the energy is conserved both in amplitude and in phase.

4.3 Surface-wave cloaking

Surface waves exists at the interface between different electromagnetic media such as: stratified planar structures or even more complicate curved surfaces. Controlling them in complex geometrical environments is of great importance, especially for communications (absorption, radiation, invisibility cloaks) and sensing applications [27]. Approaches used in the past suffer of several drawbacks: they are dependent on the geometry/shape of the object, not very suited for electrically large dimensions, rely on material properties not easy to realize. In this paragraph we focus our attention on the applications of curvilinear MetaSurfaces for surface-waves cloaking. find lots of applications in cloaking devices. The aim of the MetaSurface cloak is to render the object deposited underneath

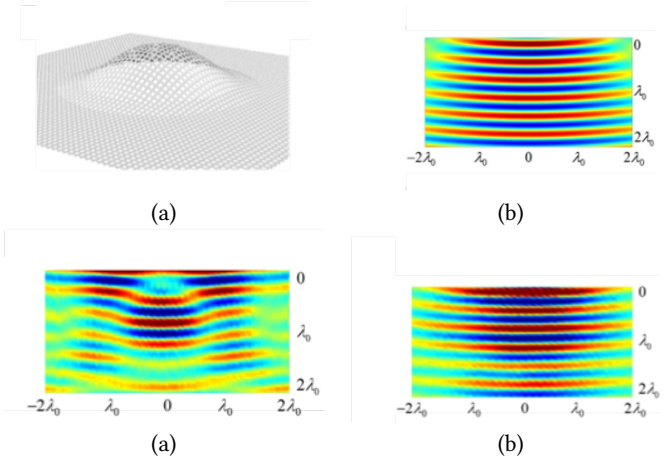

Figure 6: (a) Curvilinear MetaSurface realized for Surface-Wave Cloaking. 2D experimental electric field distribution for: (b) Flat case (Reference Sample); (c) Homogeneous Dielectric Slab (No-Cloak Sample); (d) Curvilinear MetaSurface (Cloak Sample).

transparent to the impinging electromagnetic wave, letting the waves propagate undisturbed along their path.

For the cloak, to replicate the EM configuration of the source, the following curvilinear (r, θ, ϕ) Impedance distribution has been designed and realized (Figure 6 (a)) [11]:

$$\alpha_{planar-spherical} = \begin{pmatrix} r^2 \sin\theta & r\sin\theta & r\sin\theta \\ r\sin\theta & \sin\theta & 1 \\ r & 1 & \frac{r}{\sin\theta} \end{pmatrix}. \quad (8)$$

For the experimental validation, three different samples are considered and compared: (*i*) a flat grounded dielectric slab with homogeneous permittivity as reference, (*ii*) the metallic object under the same homogeneous permittivity layer, and (*iii*) the metallic object covered with the Impedance distribution here evaluated. The performance results of the realized structure is depicted in Figure 6 (b), Figure 6 (c) and Figure 6 (d) for the flat, no-cloak and cloak, respectively. For the Cloak case, the subunits are arranged so close to each other like a net, leading to a well-confined electric field in the dielectric gaps. The intra-layer coupling effects are due to mutual impedances among adjacent unit-cells generated by the tangential components of both electric and magnetic fields along the surface: both Capacitive (X_c) and Inductive (X_L) elements are the dominant terms in the non-homogeneous Impedance distribution. Such elements are responsible for the correct reconstruction of both amplitude and phase of the surface-wave with no shadow and the object is cloaked.

5 CONCLUSIONS

In this work, a new method to realize curvilinear MetaSurface for light control and manipulation has been presented. Such approach creates a robust link between arbitrary shape structures and their analogue material properties in an intuitive manner. As a proof of concept, a MetaSurface structure has been designed, manufactured and experimentally tested for sensing, communications and cloaking applications. The tests performed revealed the capability of the MetaSurface to control simultaneously its electromagnetic properties (*i.e.*, amplitude, phase and bandwidth) and physical features (*i.e.*, materials, geometry, and dimensions). Moreover, the structure appears to be versatile and most importantly scalable for different frequency ranges and sizes. The proposed design and manufacturing approach can be applied to other industrial applications that are described via wave equations beyond electromagnetics, such as acoustics, fluid-dynamics and heat propagation.

REFERENCES

[1] C. Liaskos, S. Nie, A. Tsioliaridou, A. Pitsillides, S. Ioannidis, and I. Akyildiz, "A New Wireless Communication Paradigm through Software-controlled Metasurfaces," *IEEE Communications Magazine*, vol. 56, no. 9, pp. 162-169, 2018.
[2] C. Liaskos, A. Tsioliaridou, A. Pitsillides, S. Ioannidis, and I. Akyildiz, "Using any Surface to Realize a New Paradigm for Wireless Communications," *Communications of the ACM*, vol. 61, no. 11, pp. 30-33, 2018.
[3] J. B. Pendry, D. Schurig and D. R. Smith, "Controlling electromagnetic fields," *Science* 312, 1780-1782, 2006.
[4] W. Cai, and V. Shalaev, "Optical Metamaterials: Fundamentals and Applications," (Heidelberg: SpringerVerlag), 2010.
[5] N. I. Zheludev, "The Road Ahead for Metamaterials," *Science* 328, 582-583, 2010.
[6] C.L. Holloway, *et al.* "An overview of the theory and applications of metasurfaces: The two-dimensional equivalents of metamaterials," *IEEE Antennas Propag. Mag.*, 54, 10-35, 2012.
[7] A. Li, S. Singh and D. Sievenpiper, "Metasurfaces and their applications," *Nanophotonics*, 7(6), pp. 989-1011, 2018.
[8] S. Hassani Gangaraj, and F. Monticone, "Molding light with metasurfaces: from far-field to near-field interactions," *Nanophotonics*, 7(6), pp. 1025-1040, 2018.
[9] I. Liberal, Y. Li, and N. Engheta, "Reconfigurable epsilon-near-zero metasurfaces via photonic doping," *Nanophotonics* 7, 1117-1127, 2018.
[10] F. Monticone, N. M. Estakhri and A. Alú, "Full control of nanoscale optical transmission with a composite metascreen," *Phys. Rev. Lett.* 110, 203903, 2013.
[11] L. La Spada, *et al.* "Curvilinear MetaSurfaces for Surface Wave Manipulation," *Scientific Reports*, 2019.
[12] L. La Spada, "Metasurfaces for Advanced Sensing and Diagnostics," *Sensors*, 19(2), 355, 2019.
[13] P. Gay-Balmaz, and O.J.F. Martin, "Electromagnetic resonances in individual and coupled split-ring resonators," *J. Appl. Phys.*, 92, 2929-2936, 2002.
[14] J.B. Pendry, *et al.* "Magnetism from conductors and enhanced nonlinear phenomena," *IEEE Trans. Microw. Theory Tech.*, 47, 2075-2084, 1999.
[15] V. Delgado, *et al.* "Analytical circuit model for split ring resonators in the far infrared and optical frequency range," *Metamaterials*, 3, 57-62, 2009.
[16] F. Qin, *et al.* "Hybrid bilayer plasmonic metasurface efficiently manipulates visible light," *Sci. Adv.*, 2 (1501168), 2016.
[17] L. La Spada, *et al.* "Surface wave cloak from graded refractive index nanocomposites," *Sci. Rep.*, 6, 22045-22322, 2016.
[18] H. Tao, *et al.* "Metamaterials on paper as a sensing platform," *Adv. Mater.*, 23, 3197-3201, 2011.
[19] S. Gabriel, "The dielectric properties of biological tissues," *Phys. Med. Biol.*, 41, 2271-2293, 1996.
[20] Bingham, *et al.* "Planar wallpaper group metamaterials for novel terahertz applications," *Opt. Express*, 16, 18565-18575, 2008.
[21] L. La Spada and L. Vegni, "Electromagnetic nanoparticles for sensing and medical diagnostic applications," *Materials*, 11, 603, 2018.
[22] ME Candela, *et al.* "Resident mesenchymal progenitors of articular cartilage," *Matrix Biology* 39, 44-49, 2014.
[23] S. Asai, *et al.* "Tendon Progenitor Cells in Injured Tendons Have Strong Chondrogenic Potential: The CD 105-Negative Subpopulation Induces Chondrogenic Degeneration," *Stem Cells* 32 (12), 3266-3277, 2014.
[24] M. Lindemann *et al.*, "Ultrafast spin-lasers," *Nature* 568, 212-215, 2019.
[25] C.A. Balanis, "Advanced Engineering Electromagnetics," John Wiley & Sons: Hoboken, NJ, USA, 1999.
[26] L. La Spada and L. Vegni, "Near-zero-index wires," *Opt. Express* 25, 23699-23708, 2017.
[27] L. La Spada, S. Haq, and Y. Hao, "Modeling and design for electromagnetic surface wave devices," *Radio Sci.*, 52, 1049-1057, 2017.